

RESEARCH

Open Access



# Control of opening duration in a pneumatically operated valve with two-fluid combination and quadratic damping

Debanjan Das<sup>1\*</sup> , Shrey Waghmare<sup>1</sup>, P. Padmanabhan<sup>1</sup>, V. Kumaresan<sup>1</sup> and D. P. Sudhakar<sup>1</sup>

\*Correspondence:  
debanjan.iiests@gmail.com

<sup>1</sup> Systems Reliability Group, ISRO Propulsion Complex, Indian Space Research Organisation, Tirunelveli, Tamil Nadu (Mahendragiri) 627133, India

## Abstract

In this paper, opening characteristics of a pneumatically operated valve and methodology for controlling the valve opening duration have been investigated through numerical simulation. The valve has a poppet mounted with spring which is actuated by a pneumatic command pressure to provide a displacement of 30 mm in fully open condition. The spring housing comprises of columns of two fluids, namely air and oil, and an orifice which communicates with an adjacent auxiliary chamber. As the poppet is actuated, air initially passes through the orifice leading to a fast opening of the valve. Subsequently, opening rate of the valve is reduced as oil column encounters the orifice. The governing differential equations of motion for the valve poppet were solved using a fourth-order Runge–Kutta method, and the resistance offered by the orifice to oil flow was considered using a quadratic damping model. Simulations were carried out for two different orifice sizes, and results were validated with experiments. It was noted that for the same valve assembly, the opening duration can be controlled by varying the length of oil column and/or the orifice diameter, with no change in command pressure.

**Keywords:** Pneumatic valve, Controllable valve opening rate, Quadratic damping, Orifice-induced control, Two-fluid actuator, Runge-Kutta method

## Introduction

Valves form an important component in almost all industrial fluid systems. Major applications include isolation of fluid circuits, pressure regulation/flow control (by acting as flow resistance elements), and transient response control in dynamic systems where the valve opening/closing characteristics may significantly influence system performance.

There exist several types of valves, classified based on configuration (poppet valve, ball valve, gate valve, globe valve, butterfly valve, etc.); opening characteristics (valves having quick opening, linear or equal percentage opening characteristic); response time (fast opening and slow opening valves); method of actuation (pneumatic, motorized, etc.); and mode of operation (full open-full close type isolating valve, control valve, nonreturn valve, etc.). In this paper, a particular design of a pneumatically operated poppet valve has been studied. The valve employs variable rate of opening (a

fast opening phase followed by a slower one), thus enabling regulation of fluid velocity and acceleration in the fluid circuit in which the valve is used. This aids in applications where the fluid encounters a flow-resisting element immediately after the valve and high flow acceleration, if not controlled, may lead to pressure surge in fluid lines, often causing structural failure during transient phase [1–3]. Also, these may be used for regulated pressurization and/or filling of fluid circuits. Such applications can be noted for propellant admission valves in liquid rocket engines which require controlled flow of propellants in combustion chamber to achieve a specific mixture ratio (ratio of mass of oxidizer and fuel) during ignition so that hot start is prevented [3].

Valves with variable opening rates may also facilitate need-based online modification of system dynamic response. An example of such kind is the turbine bypass valve used in coal-based thermal power plant with steam as working fluid. The power output of the turbine remains in accordance with the power demand which the generating station has to cater. When the demand drops, power output of the turbine is reduced by decreasing steam flow from boiler to turbine through controlled closing of steam flow governing valves at turbine inlet. During transient, as the steam flow decreases, steam pressure in boiler tends to increase. To prevent pressure rise above allowable limits, bypass valves are provided through which the excess steam at boiler outlet is dumped directly into condenser bypassing the turbine. Based on whether the power demand drops suddenly or gradually, these bypass valves should have opening rates ranging from very fast opening to gradual opening respectively to ensure system safety. Although such setup can be realized by using multiple valves with different opening rates connected in parallel and operating either of these based on requirement [4, 5], an alternative may be proposed based on the present study for using and controlling a single valve capable of providing multiple opening rates.

Also, in applications where a valve in closed condition isolates fluid at two different temperatures in the upstream and downstream side, valve opening rate may play an important role in regulating mixing of the fluids and, hence, controlling its temperature during transient phase. Furthermore, if valve opening is not suitably controlled, sudden flow of a very hot fluid in a relatively cold conduit may lead to thermal shock and affect the structural integrity of the piping systems [4].

The schematic configuration of the poppet valve studied in this paper is shown in Fig. 1. The valve comprises of a valve body in which a valve poppet is made to actuate. The representation as shown in the figure finds application as an isolation valve where the flow communication between valve upstream and downstream segments is prevented in valve closed condition. Sealing is achieved by means of a seat (made of a soft material such as rubber, Teflon) and further aided by the fluid pressure in the upstream segment. The seat is held between valve poppet and seat retainer. The valve poppet remains screwed with the valve stem which in turn remains connected with valve piston by fastener (the valve poppet-seat-seat retainer-valve stem-piston combination will be referred as poppet assembly hereafter). The valve body comprises of a housing in which the poppet assembly is made to slide against a compression spring upon actuation by pneumatic command. A collar is provided in the housing which limits valve displacement to the required value.

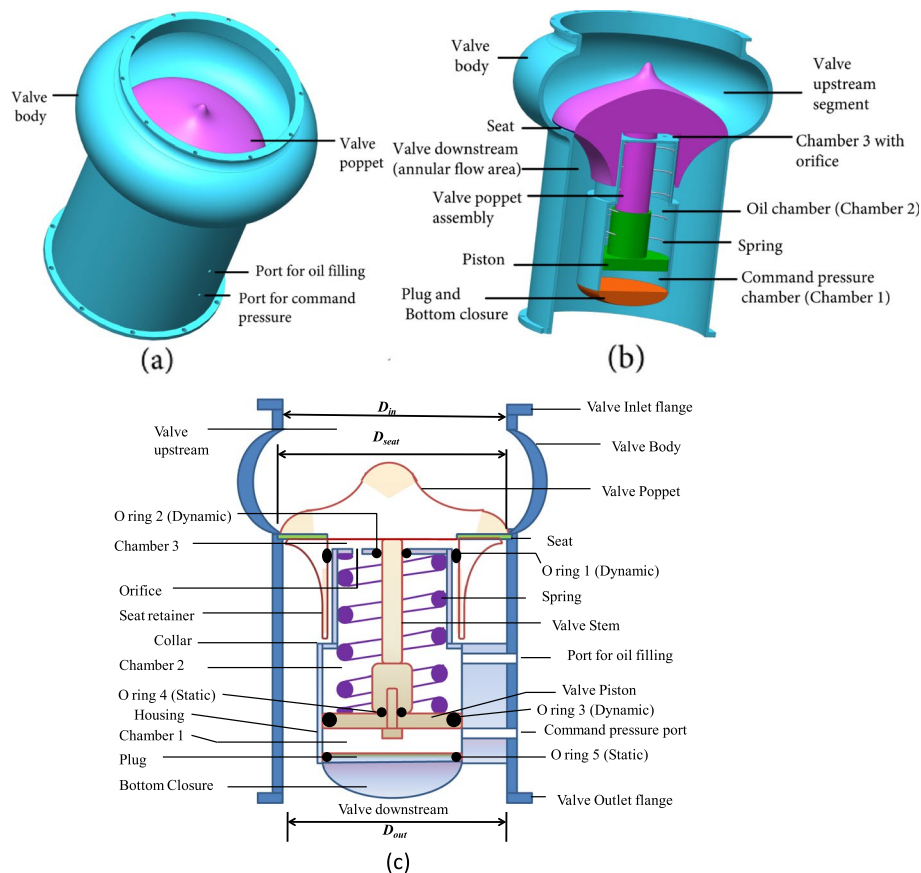


**Fig. 1** **a** 3-D model of the valve. **b** 3-D view of the valve with a cut section showing the internal components. **c** 2-D schematic configuration of valve in closed condition (sectional view)

The command pressure is applied on the piston through a command pressure port provided in the housing. The volume of the housing enclosed by piston and plug is the chamber 1 as shown in Fig. 1c, referred hereafter as command pressure chamber. This chamber remains sealed from adjacent chamber (chamber 2) and valve downstream passage through O-rings 3, 4 (dynamic O-ring at piston-housing interface and static O-ring at piston-valve stem interface respectively) and O-ring 5 (static O-ring at plug-housing interface) respectively to prevent leakage of command pressure. The plug is held in position by means of a bottom closure which remains screwed to the valve housing.

Furthermore, the valve remains equipped with two other chambers, namely, chamber 2, which contains the compression spring, and an auxiliary chamber (chamber 3) which communicates with chamber 2 through an orifice (refer to Fig. 1c). These chambers remain sealed from command chamber and the valve upstream/downstream passages in valve closed/open condition through O-rings 3, 4 and O-ring 1 (dynamic O-ring at seat retainer-housing interface) respectively. The clearance between valve stem and body housing remains sealed with a dynamic O-ring (O-ring 2). The diameter of the seat (denoted by  $D_{seat}$  in Fig. 1c) is 175 mm. The inlet and outlet diameters (denoted by  $D_{in}$  and  $D_{out}$  respectively in Fig. 1c) of the valve are 170 mm each.

There exists a provision for introducing oil/other incompressible fluid in chamber 2 through an additional port provided in the housing (referred as port for oil filling in Fig. 1c). The purpose of filling oil/other incompressible fluid is to obtain an opening rate in the later phase of valve opening, which is less than the opening rate during initial phase. The length of oil column determines and controls the duration of time for which these different opening rates remain in effect. Post oil filling, the valve configuration is shown in Fig. 2.

In the past, a lot of relevant research has been carried out to study valve’s opening and closing characteristics. Song et al. [6] carried out simulation of a spring-loaded safety relief valve by varying opening and closing parameters. The effect of change in spring stiffness was studied to decrease blowdown. Shiao et al. [7] conducted dynamic simulations on magneto-rheological valve train and concluded that the valve overlap angle can be reduced by adjusting valve opening area which in turn can effectively improve the efficiency of a crank-piston-driven internal combustion engine at low speeds. Detailed studies [8–11] have been carried out on a variety of methods to control opening rate of valves so as to cater the end system requirements. Zhang et al. [12] proposed use of a novel micro-fluidic gas damper as variable gas resistor, which changes pneumatic resistance automatically with variation of input pressure, thus facilitating variable opening area based on variable input conditions to obtain stable fluid delivery in micro-fluidic gas systems.

The effect of damping orifice in a pneumatic valve with oil as a control fluid has also been studied for various valve configurations. Wang et al. [13] proposed reduction of hydraulic impact by actively adjusting the opening size of the damping orifice. Ren et al. [14] studied the dynamic mathematical model of a Power Shift Control Valve used in construction machineries and analyzed pressure variation and buffering characteristics for load handling while carrying out shifting activities at construction sites. The study revealed that the proper matching of spring stiffness and damping orifice is essential

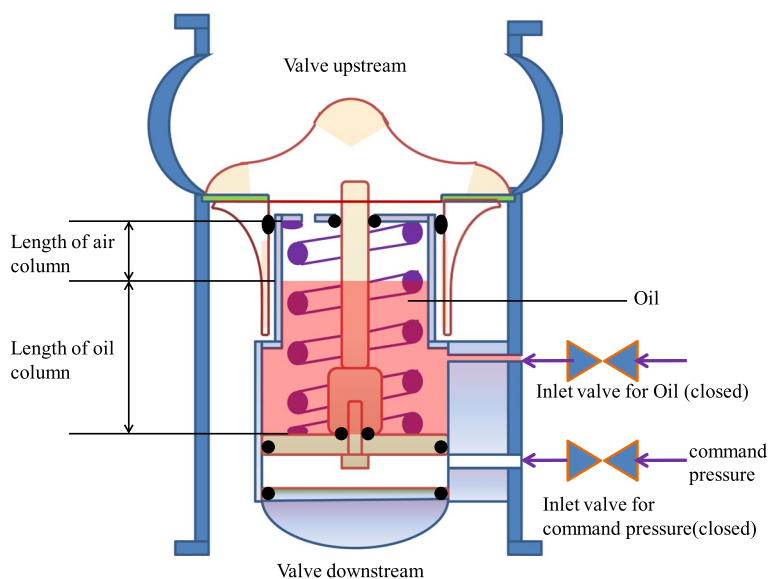


**Fig. 2** Valve in closed condition after oil filling

to meet requirements of machinery in an optimal manner. Changbin et al. [15] studied a particular case involving the phenomenon of flow ripples caused due to reverse flow resulting from pressure difference between piston chamber and orifice discharge. A flow ripple model was established, and a change in damping orifice, buffer chamber, and throttle hole was suggested to minimize the pressure difference in order to restrain flow pulsation. Zeng et al. [16] analyzed the dynamic characteristics of a motor-operated digital large flow emulsion relief valve. The influence of damping hole on dynamic response of valve spool was studied using a mathematical model involving linear viscous damping. Qian et al. [17] analyzed the effects of pilot pipe and damping orifice arrangements in pilot control globe valve (PCGV) and studied its overall flow characteristics. Zhang et al. [18] studied the phenomenon of change in opening time of seat valve by minimizing the axial flow force on the spool. The study demonstrated use of a perforated damping sleeve that affects the pressure distribution along spool cone significantly. Jang et al. [19] proposed a simple structure of the pilot pressure reduction valve (PRV) and concluded that orifice diameter and pilot lift are the important variables in opening characteristics that affect the pressure drop. Zhang et al. [20] studied the influence of different damping parameters (damping hole and middle nozzle diameters) on the opening and closing characteristics of a two-stage pressure control vent valve.

Most of the studies, as mentioned above, have been performed with respect to valve body geometry, spring and damping hole, and its effects on valve performance. However, there exists very limited research on use of two different fluids in series to control opening rate through change in relative length of the fluid columns. The same has been explored in the present study. The specific configuration, as detailed in this paper, in combination with the concept of orifice-induced damping, is capable of providing a simple yet robust and reliable design principle for a valve with variable rate of opening. Also, in contrary to the linear model for orifice-induced damping as used in the studies mentioned above, the present work employs formulation of a nonlinear mathematical model based on quadratic damping. This has been found to represent the system in a better manner as depicted by the experiments performed for model validation.

## Methods

This section deals with determination of opening rates for the valve in oil-filled condition as shown in Fig. 2. It is evident from the figure that chamber 2 has two fluid columns of air and oil. Thus, the opening of the valve upon actuation can be categorized into two phases. First phase is referred as the air-column-controlled valve opening when the valve opens at a fast rate. This begins as the inlet valve for command pressure (shown in closed condition in Fig. 2) is opened and continues until oil encounters the orifice (Fig. 3a). Second phase is the oil-column-controlled valve opening during which the opening rate gets reduced as the orifice resists oil flow from chamber 2 to chamber 3. This phase ends when piston touches the collar in valve housing and the valve becomes fully open (Fig. 3b).

It may be noted that the analysis, as detailed in the subsequent paragraphs, holds valid when the valve remains mounted in vertical configuration with valve stem axis aligned with the direction of gravitational acceleration. This ensures that the free surface of oil

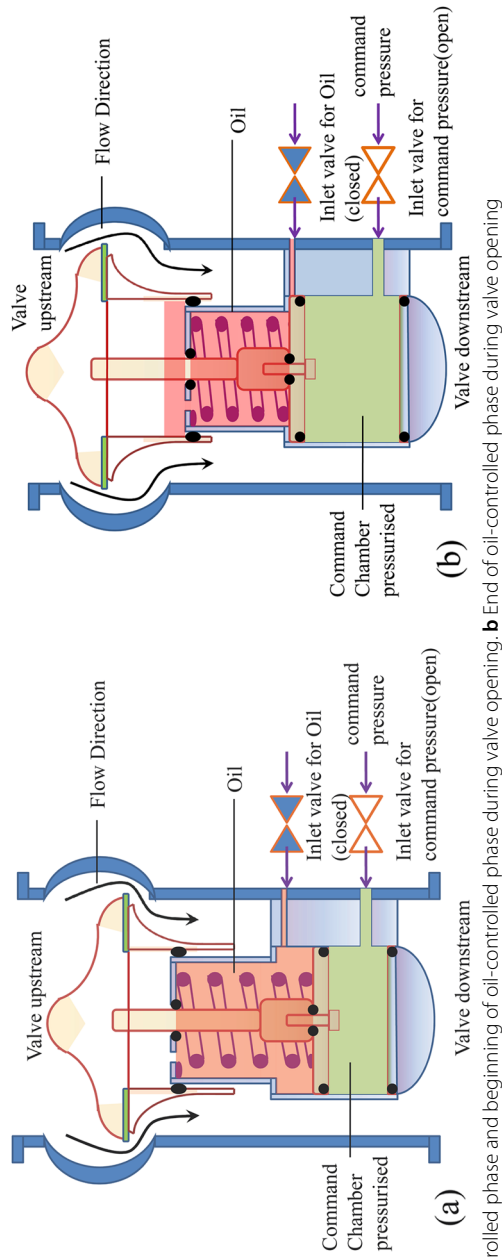


**Fig. 3** a End of air-controlled phase and beginning of oil-controlled phase during valve opening. b End of oil-controlled phase during valve opening

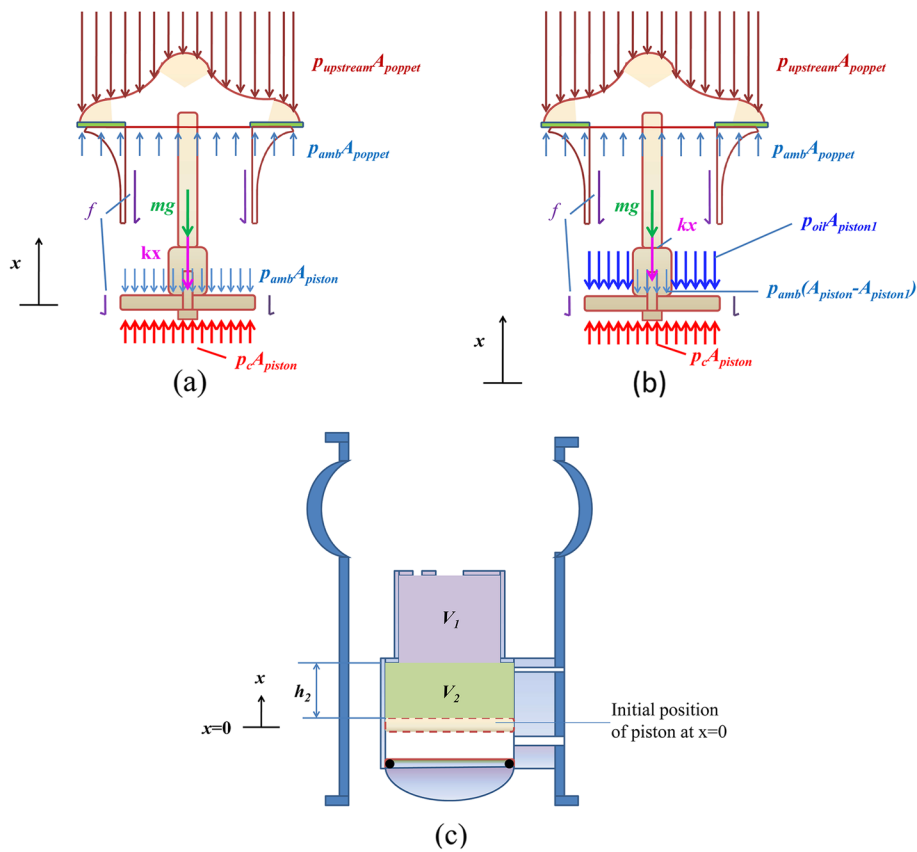


**Fig. 4** **a** Free body diagram during air-controlled phase of valve opening. **b** Free body diagram during oil-controlled phase of valve opening. **c** Housing compartment volume divided into  $V_1$  and  $V_2$  for illustration

remains perpendicular to the orifice flow axis. Also, during the transient phase when the valve opens, valve downstream is maintained at ambient conditions.

### Governing equations of motion

During first phase of valve opening, the spring starts to compress as the piston starts moving upward. The piston movement is promoted by command pressure, while it is resisted by the restoring force from spring, fluid pressure in valve upstream, and friction forces provided by the dynamic O-rings at the associated interfaces. It is assumed that the resistance provided by orifice to air flow is minor. Furthermore, the pressure on the piston due to weight of oil column remains negligible compared to the other forces involved. Hence, these have not been considered in the model. The free body diagram of the poppet assembly during first phase of valve opening is shown in Fig. 4a.

The equation of motion is written as follows:

$$m\ddot{x}(t) + k\{x(t) + x_c\} = p_{cg}(t)A_{piston} - p_{upstreamg}(t)A_{poppet} - f - mg \quad (1)$$

where  $m$  is the mass of poppet assembly,  $x$  is piston displacement,  $x_c$  is the initial spring compression (induced by hardware configuration and assembly),  $k$  is spring stiffness,  $g$  is gravitational acceleration,  $t$  is time, and  $f$  is the O-ring friction.  $p_c$  and  $p_{upstream}$  denote valve command pressure and upstream pressure respectively.  $p_{amb}$  denotes ambient

pressure.  $A_{poppet}$  is the projected area of valve poppet on which the valve upstream pressure acts.  $A_{piston}$  denotes the piston area on which the command pressure acts. Subscript “g,” wherever used, denotes gauge pressure.

During second phase of valve opening, oil flows through the orifice leading to a pressure drop across the same. The flow resistance provides an additional pressure on the piston  $p_{oil}$  (refer to Fig. 4b) retarding its upward motion and hence reducing the opening rate of the valve. The pressure drop across the orifice can be computed from the energy equation for fluid flow as follows:

$$p_{oil} - p_{amb} = \frac{\rho_{oil}}{2} \left( \frac{1}{C_d A_{or}} \right)^2 Q^2 \tag{2}$$

where  $\rho_{oil}$  is oil density,  $C_d$  is the orifice discharge coefficient,  $A_{or}$  is the orifice flow area, and  $Q$  is the volume flow rate of oil passing out through the orifice. The volume flow rate  $Q$  may be obtained from the mass conservation equation as follows:

$$Q = -\frac{dV_{oil, chamber2}}{dt} = -\frac{d}{dt} (V_1 + V_2 - V_{spring} - V_{stem, chamber2}) \tag{3}$$

where  $V_{oil, chamber2}$  denotes volume of oil that lies within chamber 2 at any instant (after onset of oil-controlled phase),  $V_1$  denotes volume of chamber 2 located below top wall (which contains orifice) and above the collar, and  $V_2$  denotes volume of chamber 2 located below the collar and above the piston. This is illustrated in Fig. 4c.  $V_{spring}$  is the volume of compression spring, and  $V_{stem, chamber2}$  is the volume of poppet assembly that lies within chamber 2 at any instant. Noting that  $V_1$  and  $V_{spring}$  are constants and  $A_{stem}$  is the cross-sectional area of the valve stem, the following equations can be written as:

$$V_2 = A_{piston}(h_2 - x) \tag{4}$$

$$\frac{d}{dt} (V_{stem, chamber2}) = -A_{stem}\dot{x} \tag{5}$$

Hence, from Eq. (3), the expression for the volume flow rate of oil is obtained as follows:

$$Q = (A_{piston} - A_{stem})\dot{x} \tag{6}$$

Thus, using Eq. (2), the additional retarding force on the piston exerted by oil due to orifice flow resistance is obtained as follows:

$$F_{oil, piston} = p_{oil}A_{piston1} = p_{amb}A_{piston1} + c_{oil}\dot{x}^2 \tag{7}$$

where  $A_{piston1}$  is area of the piston on which the oil pressure acts (refer to Fig. 4b).  $c_{oil}$  represents the effective damping coefficient due to resistance provided by orifice to oil flow. Using Eq. (2) and Eq. (6), the same may be expressed as follows:

$$c_{oil} = \frac{\rho_{oil}A_{piston1}}{2} \left( \frac{A_{piston} - A_{stem}}{C_d A_{or}} \right)^2 \tag{8}$$



From the free body diagram during second phase of valve opening as shown in Fig. 4b, the equation of motion for the poppet assembly is written as follows:

$$m\ddot{x}(t) + k\{x(t) + x_c\} + p_{oil}A_{piston1} + p_{amb}(A_{piston} - A_{piston1}) = p_c(t)A_{piston} - p_{upstream}(t)A_{poppet} - f - mg \tag{9}$$

Using Eq. (7), Eq. (9) can be reframed as follows:

$$m\ddot{x}(t) + c_{oil}\dot{x}(t)^2 + k\{x(t) + x_c\} = p_{cg}(t)A_{piston} - p_{upstream}(t)A_{poppet} - f - mg \tag{10}$$

**Numerical solution**

The governing equations of motion during first and second phase of valve opening, as represented by Eq. (1) and Eq. (10), respectively, can be cast in a general form as follows:

$$m\ddot{x} + c\dot{x}^2 + kx = F(t) \tag{11}$$

where  $c=0$  during first phase [damping coefficient due to airflow through orifice  $c_{air} < c_{oil}$  as per Eq. (8) owing to the fact that the density of air is much less than that of oil] and  $c=c_{oil}$  during second phase of valve opening. Also,  $F(t)$  takes into account the time-varying forces due to varying valve upstream pressure (this varies in course of valve opening as the flow takes place from upstream to downstream segment of valve) and command pressure. This is given as follows:

$$F(t) = p_{cg}(t)A_{piston} - p_{upstream}(t)A_{poppet} - f - mg - kx_c \tag{12}$$

It is evident from Eq. (11) that the damping term in the equation of motion is quadratic in nature and has a nonzero value for oil-controlled phase of valve opening which renders the differential equation non-linear. The second-order ordinary differential equation (ODE) has been solved using a fourth-order Runge–Kutta method as follows (implementation of the scheme has been detailed further in Appendix A).

The second-order ODE is first decomposed into two first-order ODEs  $v(x,t)$  and  $a(x,v,t)$  where  $v$  and  $a$  represent velocity and acceleration respectively.

$$\frac{dx}{dt} = \dot{x} = v(x, t) \tag{13}$$

$$\frac{dv}{dt} = \frac{F(t) - kx - cv^2}{m} = a(x, v, t) \tag{14}$$

This is a set of simultaneous first-order differential equations with two dependent variables,  $x$  and  $v$ , which represent poppet assembly displacement and velocity respectively. Time  $t$  is the only independent variable. If  $h$  is the time-step interval after which the variables  $x$  and  $v$  are to be calculated, assuming  $x_0$  and  $v_0$  to be the known initial values for variables  $x$  and  $v$  respectively at the beginning of time step  $t_0$  (equivalent to point A in Fig. A1, Appendix A), the values  $x_1$  and  $v_1$  (values for variables  $x$  and  $v$  respectively at end of the time step  $t_0 + h$ ; equivalent to point E in Fig. A1, Appendix A) are calculated as follows:

$$x_1 = x_0 + \frac{1}{6}(K_{1x} + K_{2x} + K_{3x} + K_{4x})h \tag{15}$$

$$v_1 = v_0 + \frac{1}{6}(K_{1v} + K_{2v} + K_{3v} + K_{4v})h \tag{16}$$

where  $K_x$  and  $K_v$  represent slopes of  $x$  and  $v$  with respect to  $t$  respectively calculated at various intermediate points during implementation of Runge–Kutta scheme (for details, see Appendix A). The slopes  $K_x$  and  $K_v$  at beginning of the time step are calculated [using Eqs. (13 and (14)] respectively at  $(x_0, v_0, t_0$ ; equivalent to point A in Fig. A1, Appendix A) as follows:

$$K_{1x} = v(x_0, t_0) = v_0 \tag{17}$$

$$K_{1v} = a(x_0, v_0, t_0) = \frac{F(t_0) - kx_0 - cv_0^2}{m} \tag{18}$$

The estimates of  $x$  and  $v$  at midpoint of the time step (time instant:  $t_0 + 0.5 h$ ; equivalent to point B in Fig. A1, Appendix A) are obtained next as follows:

$$x' = x_0 + K_{1x} \frac{h}{2} \tag{19}$$

$$v' = v_0 + K_{1v} \frac{h}{2} \tag{20}$$

The first set of mid-point slopes is then calculated at this estimated midpoint  $(x', v', t_0 + 0.5 h$ ; equivalent to point B in Fig. A1, Appendix A) [using Eqs. (13 and (14)] as follows:

$$K_{2x} = v\left(x', t_0 + \frac{h}{2}\right) = v' \tag{21}$$

$$K_{2v} = a\left(x', v', t_0 + \frac{h}{2}\right) = \frac{F(t_0 + 0.5h) - kx' - cv'^2}{m} \tag{22}$$

Based on this, the mid-point predictions for  $x$  and  $v$  (time instant:  $t_0 + 0.5 h$ ; equivalent to point C in Fig. A1, Appendix A) are revised as follows:

$$x'' = x_0 + K_{2x} \frac{h}{2} \tag{23}$$

$$v'' = v_0 + K_{2v} \frac{h}{2} \tag{24}$$

The second set of mid-point slopes is then calculated at this estimated midpoint  $(x'', v'', t_0 + 0.5 h$ ; equivalent to point C in Fig. A1, Appendix A) [using Eqs. (13 and (14)] as follows:

$$K_{3x} = v \left( x'', t_0 + \frac{h}{2} \right) = v'' \tag{25}$$

$$K_{3v} = a \left( x'', v'', t_0 + \frac{h}{2} \right) = \frac{F(t_0 + 0.5h) - kx'' - cv''^2}{m} \tag{26}$$

The predictions at end of the interval (time instant:  $t_0 + h$ ; equivalent to point D in Fig. A1, Appendix A) are determined as follows:

$$x''' = x_0 + K_{3x}h \tag{27}$$

$$v''' = v_0 + K_{3v}h \tag{28}$$

The endpoint slope estimates are determined at this estimated endpoint ( $x''', v''', t_0 + h$ ; equivalent to point D in Fig. A1, Appendix A) [using Eqs. (13 and 14)] as follows:

$$K_{4x} = v \left( x''', t_0 + h \right) = v''' \tag{29}$$

$$K_{4v} = a \left( x''', v''', t_0 + h \right) = \frac{F(t_0 + h) - kx''' - cv'''^2}{m} \tag{30}$$

The slopes  $K_{1x}$  and  $K_{1v}$  [from Eqs. (17) and (18), respectively];  $K_{2x}$  and  $K_{2v}$  [from Eqs. (21) and (22), respectively];  $K_{3x}$  and  $K_{3v}$  [from Eqs. (25) and (26), respectively]; and  $K_{4x}$  and  $K_{4v}$  [from Eqs. (29) and (30), respectively], as determined, are used in Eq. (15) and Eq. (16) to get final values for  $x_1$  and  $v_1$  (time instant:  $t_0 + h$ ; equivalent to point E in Fig. A1, Appendix A), i.e., poppet displacement and velocity respectively at end of the time step. This in turn can be used as the known initial values for next time step, and the computation procedure can be executed in a similar way. Thus, the values for displacement and velocity of the valve poppet can be determined during both phases of valve opening.

The initial conditions for the first phase of valve opening are  $x=0$  and  $v=0$ , at  $t=0$ . The computations, as detailed above, are continued until  $x = x_{air}$ , i.e., initial length of the air column in valve closed condition (refer to Fig. 2). This marks the completion of the

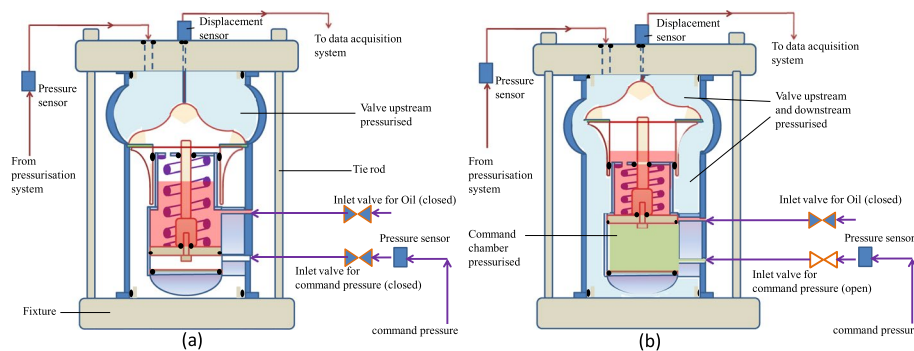


**Fig. 5** Schematic representation of experimental setup for determination of valve opening rate. **a** Valve remains in closed condition at the beginning of test. **b** Both upstream and downstream chambers of valve pressurized to 5 bar (absolute pressure) at end of the test

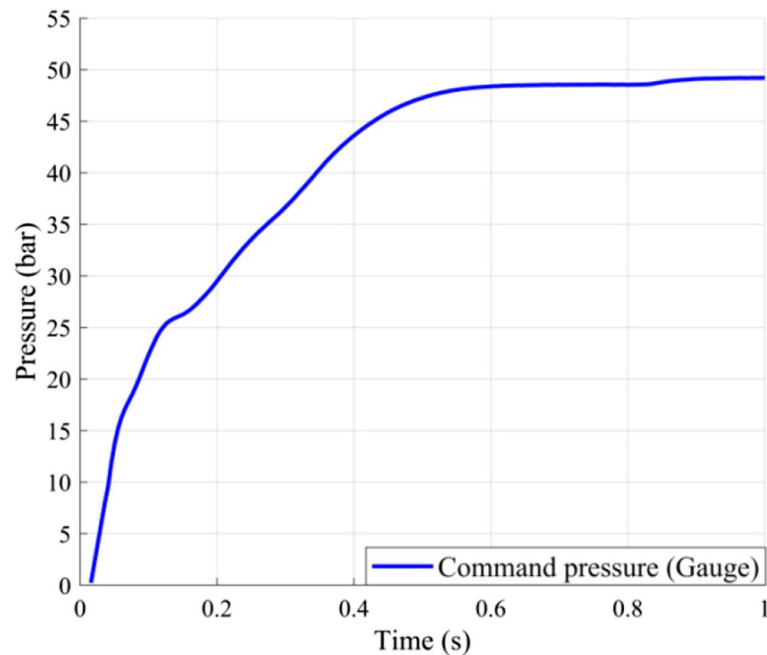


**Fig. 6** Command pressure profile

first phase of valve opening. For the second phase of valve opening, the initial condition for displacement remains as  $x = x_{\text{air}}$ . For velocity, the initial condition is given as  $v = 0$ . The computations are made until  $x = x_{\text{stroke}}$ , i.e., the piston displacement  $x$  reaches 0.03 m. At full stroke, the valve becomes fully open, and the computations for second phase of valve opening end.

It may be noted that at the transition point of first and second phase of valve opening, there is an instantaneous change in acceleration of the valve poppet due to a sudden change in net force acting on the piston. This leads to a jerk when the third-order derivative of displacement with respect to time tends to infinity (since there is a finite change in acceleration in an infinitesimally small time). The consideration of jerk has been kept outside the scope of the paper. However, it is evident that the top surface of oil moves with same velocity as that of the piston during first phase of valve opening. At the end of first phase, oil at the surface comes to rest as it encounters top wall of the housing except a very minor part of the oil surface which finds a way through the orifice. Since oil is an incompressible fluid, the information of the oil surface velocity becoming zero propagates instantaneously to the piston as a compression wave. Thus, the piston is almost brought to rest for an instant which justifies using  $v = 0$  as the initial condition at onset of the second phase of valve opening.

#### Experimental determination of valve opening rate

The setup and test process for determination of valve opening rate are detailed in Fig. 5. The valve is assembled to a fixture in which the valve upstream and downstream remain sealed from the external ambient through O-rings assembled at valve-fixture interface.

The quantity of oil in the valve is set such that the initial length of air column in the valve is about 15 mm in valve closed condition.

The valve upstream is pressurized to 5 bar (absolute pressure) with gaseous nitrogen. Subsequently, the command pressure is applied through command port for actuation of the valve. The variation of command pressure with time is determined by the command pressurization module, and the pressure profile used for the test is shown in Fig. 6.

As the valve starts opening, the upstream pressure leaks into the downstream side. The variation of valve upstream pressure depends on the design of valve body and poppet as these primarily control the valve flow area in course of valve opening. For the present case, as the valve opens, valve upstream pressure is maintained fairly constant through regulated inflow of gas in valve upstream chamber from the pressurization system. This is also confirmed by a pressure transducer connected at valve upstream end. The test continues for a duration of time which is required to bring the pressure of both upstream and downstream chamber of the valve to 5 bar (absolute). However, opening of the valve takes place faster with duration of less than a second, and during this transient, complete filling of downstream chamber to the required pressure does not take place. Hence, in the mathematical model, the pressure (absolute) on downstream side of valve poppet (in the area that remains encircled by seat retainer) has been considered as 1 bar (atmospheric ambient pressure) during both phases of valve opening.

Here, it may be noted that the total pressure exerted by the fluid on valve poppet (upstream side) has been taken as the static pressure of 5 bar (absolute) in the upstream chamber. However, as flow is induced with opening of the valve, dynamic pressure caused by fluid flow also contributes to the determination of total pressure. The flow occurring across the valve seat will be maximum when the valve immediately starts to open (since maximum differential pressure exists across the valve seat) and will reduce

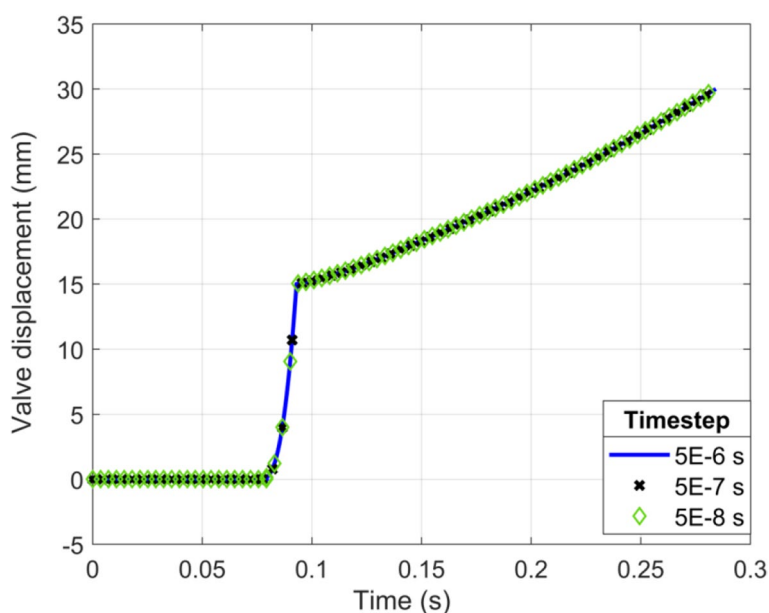


Fig. 7 Determination of optimal time step size for Runge–Kutta iterations

thereafter (as the upstream and downstream pressure equalizes). Hence, maximum dynamic pressure will also be encountered corresponding to this maximum flow at a differential pressure of 4 bar across valve seat.

For calculation of dynamic pressure, the fluid velocity considered is that with respect to the valve poppet. This has been determined as the sum of absolute velocity of fluid across valve seat (in laboratory reference frame) and the upward velocity of valve poppet (in laboratory reference frame, as determined from the opening rate graph of Fig. 9).

As noted from Fig. 3, as the valve opens, flow first passes through the annular area between seat and body (equivalent to throat in nozzle flow) and subsequently into the downstream cavity. The upstream area being higher than the throat and downstream area flow will become choked if downstream pressure is less than the sonic pressure, assuming flow in the upstream side to be isentropic.

Based on upstream pressure of 5 bar, the sonic pressure is found to be 2.64 bar. Since the downstream ambient pressure of 1 bar is less than sonic pressure, the maximum flow rate across the valve can be calculated by using choked flow relation. This has been estimated as 16.73 kg/s. Corresponding to this mass flow rate, flow velocity (relative to the poppet) has been calculated in the upstream section which yields a value of 53.92 m/s. The corresponding dynamic pressure is estimated as 0.065 bar. Since this is very less compared to the absolute pressure of 5 bar in the upstream, dynamic pressure due to flow has not been considered for the study. Also, based on the fact that gases have very less viscosity, it has been assumed that the flow induced will be inviscid. Hence, wall shear stresses induced by flow have also been neglected in the present study. However, the effect of dynamic pressure and wall shear stress needs to be considered if the test fluid had been a liquid instead of gas (gaseous nitrogen is the test fluid in the present study) due to considerable higher density and viscosity.

The orifices used for the test were threaded fitments which can be screwed in a slot made for orifice assembly in the valve housing top wall. Tests were conducted for two different orifice sizes (with diameter 2 mm and 4 mm), and a linear voltage differential transformer (LVDT) (range 0–50 mm; accuracy: 0.4% of range) was used to acquire valve displacement data (1 sample is acquired for every 0.005 s).

## Results and discussion

For computation by Runge-Kutta method, time step was considered as  $5 \times 10^{-6}$  s which was determined based on the fact that further reduction of time step (to the order of  $10^{-7}$  to  $10^{-8}$  s as shown in Fig. 7) increased the computation cost but did not improve the obtained results. For the study, cumulative friction due to dynamic O-rings was obtained experimentally. To determine  $f$ , a simple test was carried out in which air pressure was slowly given to command chamber (chamber 1 in Fig. 1). During this test, both valve upstream and downstream were maintained at ambient pressure. As long as the poppet assembly does not move, pressure keeps on increasing in the command chamber (chamber 1 in Fig. 1). As soon as it starts to move, the pressure suddenly drops a little as volume of the command chamber starts to increase. On monitoring the pressure in chamber 1, the point at which it dips has been determined. This particular pressure is just enough to overcome the friction and weight of the poppet assembly (spring was not assembled in the valve for this test). The weight being known, the frictional force was

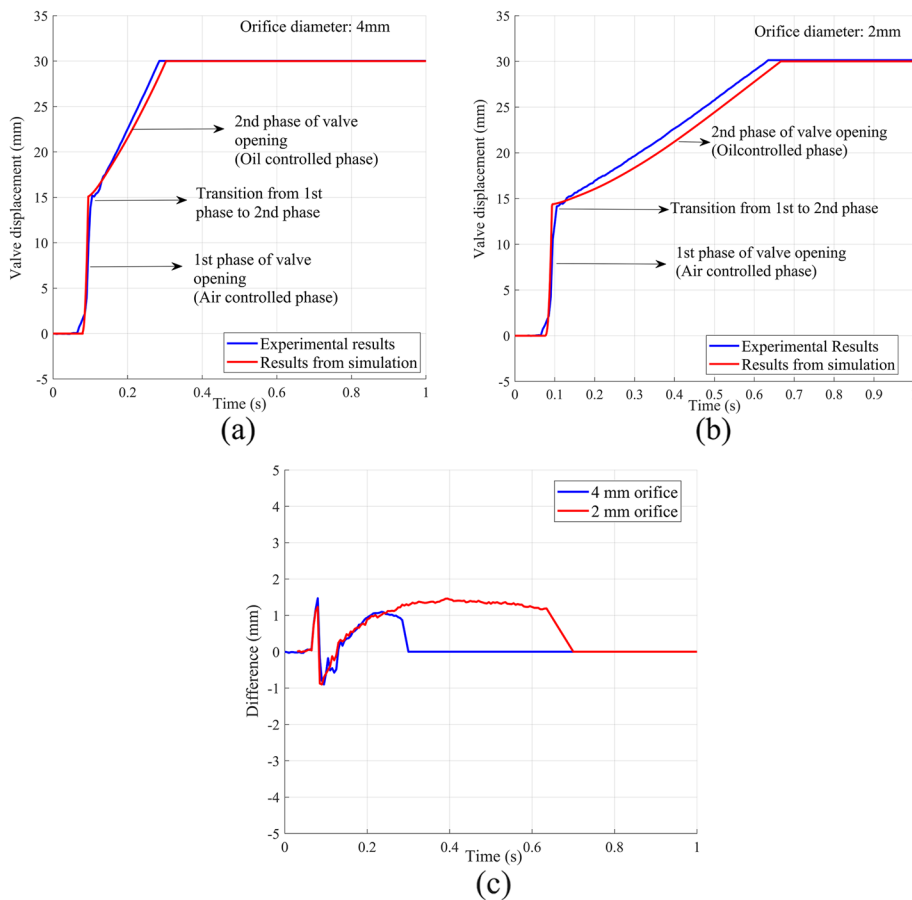


**Fig. 8** Comparison of results for valve displacement as obtained from experiment and numerical simulation. **a** For orifice with diameter 4 mm. **b** For orifice with diameter 2 mm. **c** Difference between results obtained from simulation and experiment

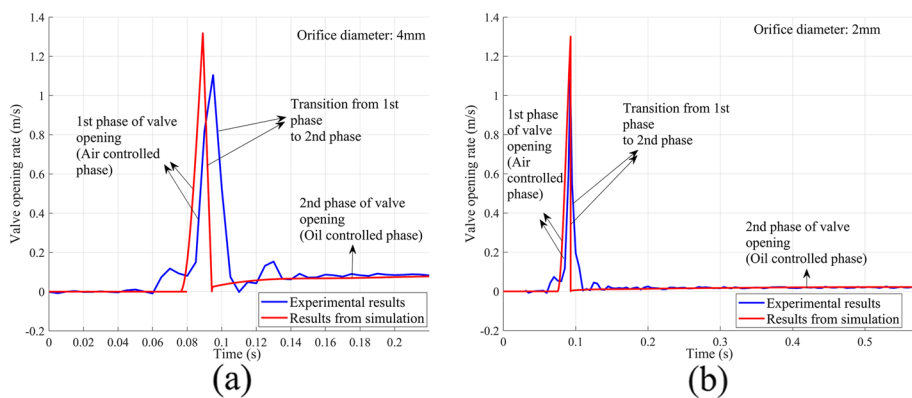


**Fig. 9** Comparison of results for valve opening rate as obtained from experiment and numerical simulation. **a** For orifice with diameter 4 mm. **b** For orifice with diameter 2 mm

estimated based on force balance, and the value obtained was 38 N. The obtained values were also validated with the available empirical co-relations which determine O-ring friction based on O-ring compression, O-ring material, and tribological parameters of

**Table 1** Comparison of results for valve opening duration as obtained from experiment and simulation

Orifice diameter (mm)	Command pressure (gauge) at which the valve starts to open (bar)		Duration of valve opening (s)	
	Experiment	Simulation	Experiment	Simulation
4	17.63	18.32	0.2212	0.2216
2	17.72		0.5708	0.5776

**Table 2** Comparison of results for valve opening rate as obtained from experiment and simulation

Orifice diameter (mm)	Opening rate at the end of 1st phase (m/s)		Opening rate during second phase (m/s)	
	Experiment	Simulation	Experiment	Simulation
4	1.1	1.31	0.09	0.08
2	1.08		0.02	0.02

the body surface. The spring used for the test has a linear force–displacement relationship. Stiffness value was measured as 77,000 N/m.

Results obtained from experiments were compared with those obtained from numerical simulation, and a good match was obtained as shown in Fig. 8. Valve opening rate (poppet velocity) as obtained from experiment (not measured directly, derived by differentiation of displacement–time data) and simulation, for both orifice sizes, have been plotted in Fig. 9. This shows that the opening rate increases during 1st phase of valve opening and remains constant during 2nd phase of valve opening. The transition is characterized by the opening rate reducing to zero for a very short period of time when oil encounters the housing top wall, as discussed earlier and further validated by experiments. The comparison of valve opening duration and opening rate, as obtained from experiments and simulation, is presented in Tables 1 and 2, respectively.

It is noted that the valve opens faster with an increase in orifice diameter since there is a reduction in flow resistance. Taking the case with orifice diameter of 4 mm as reference, there is an increase in valve opening duration by 2.58 times when the orifice diameter is reduced by 50%.

Estimation of valve opening duration by numerical model provides an absolute error of 0.18% and 1.2% for orifice diameter of 4 mm and 2 mm, respectively, when compared with the experimental results. This is attributed to the limitation of the mathematical model to simulate jerk during transition of the two phases for valve opening, uncertainties in estimation/measurement of friction/spring stiffness, oil density, accuracy of LVDT, and efficacy of the numerical method [21]. It may be noted from Fig. 8c that for first phase of valve opening, during an initial displacement of 1.5 mm, the slope of displacement curve as obtained from experiment differs slightly from that obtained through simulation. This is due to the fact that the Teflon seat used in valve remains formed and compressed in the valve closed condition. As the valve begins to open, there is a certain amount of elastic recovery when the seat starts losing contact. The stress relieving in Teflon and resulting elastic recovery leads to slight expansion (seat edge



**Table 3** Effect of various parameters on valve opening duration

Parameter	Amount by which the parameter is varied	Effect on valve opening duration
Initial length of air column (in valve closed condition) (mm)	Reduced by 10%	Increased by 6.04%
	Reduced by 30%	Increased by 17.55%
	Reduced by 50%	Increased by 28.38%
Oil density (kg/m <sup>3</sup> )	Reduced by 10%	Reduced by 3.87%
	Reduced by 30%	Reduced by 11.56%
	Reduced by 50%	Reduced by 20.81%
Spring stiffness (N/m)	Reduced by 10%	Reduced by 1.19%
	Reduced by 30%	Reduced by 3.38%
	Reduced by 50%	Reduced by 5.46%
Upstream pressure (bar)	Reduced by 10%	Reduced by 3.31%
	Reduced by 30%	Reduced by 11.62%
	Reduced by 50%	Reduced by 19.28%

**Table 4** Minimum and maximum valve opening duration achievable with 4-mm diameter orifice

Initial condition in chamber 2	Valve opening duration (s) (with 4-mm diameter orifice)
No oil in chamber 2	0.024
Chamber 2 fully filled with oil (in valve closed condition)	0.336

continues to remain in contact with side walls of valve body) for which loss of contact of the seat from valve body is not instantaneous but dwells over a brief period of time up to a piston displacement of about 1.5 mm. This contributes to some additional frictional resistance which results in slightly less opening rate in this regime. Also, from Fig. 8c, for the second phase of valve opening, it is noted that the displacement curve as obtained from simulation deviates from that obtained through experiment at the transition point after which both curves become parallel. The deviation is attributed to the flow unsteadiness and jerk at the transition point which the mathematical model could not capture due to steady oil flow assumptions [use of Bernoulli's equation to estimate  $p_{oil}$  as per Eq. (2)]. The curves becoming parallel is confirmed by the close match obtained between observed (from experiment) and predicted (from simulation) opening rates as shown in Fig. 9 and tabulated in Table 2. Furthermore, the reduction in poppet velocity during oil-controlled phase ensures that there is minimum jerk at the instance when the poppet comes to rest in fully open condition of the valve.

Here, it may be mentioned that the equation for obtaining  $p_{oil}$  as represented by Eq. (2) is based on Bernoulli's equation for fluids which assumes the flow to be in steady state and along streamlines, without friction. As noted from Fig. 9, the opening rate during oil-controlled phase of valve opening remains fairly constant. Thus, the volume flow rate of oil remains steady as the same is directly proportional to this opening rate as per Eq. (6). The orifices used for the experiments have smooth edges with rounded corner radii to minimize the entry and exit losses, and discharge coefficient for orifice has been considered as 0.9 in the numerical calculations. Also, length of the orifice along flow direction is kept less to minimize friction losses. A fluoro-elastomer-based oil with high viscosity was

used in the valve. The same has been chosen to ensure that the Reynold's number for flow through orifice remains below 50, and laminar streamlined flow can be ensured. These factors validate the use of Bernoulli's equation for the numerical simulation.

Hence, it was demonstrated that the mathematical model could reasonably represent the valve opening characteristics. Subsequently, the model was used for further characterization of the valve. The valve test condition with spring stiffness of 77,000 N/m, orifice diameter of 4 mm, air column length of 15 mm, oil density 1960 kg/m<sup>3</sup>, and upstream pressure of 5 bar (absolute) is taken as the standard reference. Subsequently, any one of the parameters has been varied (the required parameter has been varied one at a time, with other parameters set to standard reference test condition), and influence on valve opening duration has been studied. The results are presented in Table 3.

For a reduction in initial length of air column (increase in initial length of oil column in valve closed condition), the oil-controlled phase dominates for a longer duration which causes additional resistance to motion due to damping forces, and thus, there is an increase in opening time for the valve. For a reduction in oil density, the damping coefficient decreases as per Eq. (8). Thus, the damping force (which opposes the upward motion) also reduces, and the valve opens faster. Similarly, for a reduction in spring stiffness and/or valve upstream pressure, the corresponding forces opposing the upward movement of poppet assembly decrease, thus reducing the duration of valve opening.

Finally, the minimum and maximum opening duration which can be achieved for the valve with orifice diameter of 4 mm is computed from the numerical model and presented in Table 4.

From Tables 1 and 3, it is evident that out of all parameters which can affect duration of valve opening, impact of change in orifice diameter is most dominant followed by the change in length of oil column. It may be noted that for all the cases discussed in this section, the variation of command pressure with time during valve opening remains same as that shown in Fig. 6.

## Conclusions

In the study, modeling, realization, and experimental validation of a pneumatic valve with controllable opening duration have been demonstrated. The valve employs combination of two fluids (air and oil in the present case), the relative lengths of which can be varied to control opening duration of the valve. The other feature which was noted to influence the opening rate was the quadratic damping induced due to flow of oil through the orifice which also enabled a smooth termination of valve opening as the piston achieved its required stroke. A numerical model of the valve opening has been formulated by solving the governing differential equations of motion by a fourth-order Runge-Kutta method. The same has been used to study the effect of change in various parameters such as oil density, orifice diameter, length of oil column, spring stiffness, and valve upstream pressure on the valve opening duration. The opening time was found to be most sensitive to change in orifice diameter and oil column length. From the aspect of engineering applications, it was noted that the valve configuration is capable of providing various opening rates for a single valve assembly in accordance with response time requirement of the system where the valve is used. In principle, the online control of valve opening duration can be achieved in the valve closed condition, without any

change in command pressure system. This can be done even when the valve remains connected to an operational fluid circuit with dynamic response time requirements. The major advantage lies in the fact that the valve need not be replaced to meet requirement of a modified opening rate and hence modified system response, thus eliminating replacement downtime. Also, the need of using multiple valves with different opening rates in parallel (as stated earlier for case of turbine bypass valve) can be eliminated. For such online control of valve opening duration by change in oil column length, regulated filling/draining of oil in the valve housing can be executed through a separate oil circuit equipped with oil pump and oil inlet/outlet valves. Also, actuating mechanisms can be employed for online variation of the orifice flow area. Furthermore, with multiple insoluble incompressible fluids instead of oil, there remains a provision for obtaining multiple opening rates (instead of two opening rates as demonstrated in the present study) during valve opening phase which can be explored further in future studies.

### Abbreviations

$m$	Mass of poppet assembly (kg)
$x$	Piston displacement (m)
$\dot{x}, v$	Velocity of the piston (m/s)
$\ddot{x}, a$	Acceleration of the piston (m/s <sup>2</sup> )
$x_c$	Initial compression of the spring (induced by hardware configuration and assembly) (m)
$k$	Spring stiffness (N/m)
$g$	Gravitational acceleration (m/s <sup>2</sup> )
$x_{air}$	Initial length of the air column in valve closed condition (m)
$x_{stroke}$	The piston stroke length of 0.03 m
$f$	O-ring friction (N)
$t$	Time (s)
$p_c$	Command pressure (N/m <sup>2</sup> )
$p_{upstream}$	Valve upstream pressure (N/m <sup>2</sup> )
$p_{amb}$	Ambient pressure (N/m <sup>2</sup> )
$p_{oil}$	Oil pressure acting on the piston (N/m <sup>2</sup> )
$A_{poppet}$	Projected area of valve poppet on which the valve upstream pressure acts (m <sup>2</sup> )
$A_{piston}$	Piston area on which the command pressure acts (m <sup>2</sup> )
$\rho_{oil}$	Oil density (kg/m <sup>3</sup> )
$C_d$	Orifice discharge coefficient
$A_{or}$	Orifice flow area (m <sup>2</sup> )
$Q$	Volume flow rate of oil passing out through the orifice (m <sup>3</sup> /s)
$V_1$	Volume of chamber 2 located below top wall (which contains orifice) and above the collar (m <sup>3</sup> )
$V_2$	Volume of chamber 2 located below the collar and above the piston (m <sup>3</sup> )
$V_{spring}$	Volume of compression spring (m <sup>3</sup> )
$V_{oil, chamber2}$	Volume of oil that lies within chamber 2 at any instant after onset of oil-controlled phase (m <sup>3</sup> )
$V_{stem, chamber2}$	Volume of poppet assembly that lies within chamber 2 at any instant (m <sup>3</sup> )
$A_{stem}$	Cross-sectional area of the valve stem (m <sup>2</sup> )
$A_{piston1}$	Area of the piston on which the oil pressure acts (m <sup>2</sup> )
$c$	Damping coefficient (N s <sup>2</sup> /m <sup>2</sup> )
$c_{oil}$	Effective damping coefficient due to resistance provided by orifice to oil flow (N s <sup>2</sup> /m <sup>2</sup> )
$c_{air}$	Effective damping coefficient due to resistance provided by orifice to air flow (N s <sup>2</sup> /m <sup>2</sup> )
Subscript "g"	Wherever used, denotes gauge pressure

### Supplementary Information

The online version contains supplementary material available at <https://doi.org/10.1186/s44147-023-00207-7>.

**Additional file 1:** Appendix A.

### Acknowledgements

The authors express their gratitude to Smt. C. Sudha, Engineer, ISRO Propulsion Complex, and her team for facilitating experimental trials. The authors are also thankful to Instrumentation Team, ISRO Propulsion Complex, for providing support to acquire the data during experiments.

### Authors' contributions

DPS conceived of this study. DD and SW carried out numerical simulation and experimental trials under the guidance and supervision of PP and VK. The authors read and approved the final manuscript.

### Funding

This research did not receive any specific grant from funding agencies in the public, commercial, or not-for-profit sectors. Valve assembly, testing, and numerical simulation have been carried out at various facilities of ISRO Propulsion Complex. Permission to publish the work has been provided by ISRO Propulsion Complex, Mahendragiri.

### Availability of data and materials

The data sets (experimental and numerical results) used and/or analyzed during the present study are available from the corresponding author on reasonable request subject to approval from concerned authority at ISRO Propulsion Complex.

### Declarations

#### Competing interests

The authors declare that they have no competing interests.

Received: 30 January 2023 Accepted: 26 April 2023

Published online: 10 May 2023

### References

1. Hearn H.C. (2005) Development and application of a priming surge analysis methodology. In: Proceedings of the 41st AIAA/ASME/SAE/ASEE Joint Propulsion Conference & Exhibit, Tucson, Arizona, July 10–13, 2005. Paper no. AIAA-2005-3738. <https://doi.org/10.2514/6.2005-3738>
2. Chaudhry MH (2014) Applied hydraulic transients. Springer, New York
3. Das D, Padmanabhan P (2022) Study of pressure surge during priming phase of start transient in an initially unprimed pump-fed liquid rocket engine. *Propuls Power Res* 11(3):353–375. <https://doi.org/10.1016/j.jprr.2022.07.003>
4. Nag PK (2006) Power plant engineering. New Delhi, Tata Mc Graw Hill
5. Pondini M, Signorini A, Colla V (2017) Steam turbine control valve and actuation system modeling for dynamics analysis. *Energy Procedia* 105:1651–1656. <https://doi.org/10.1016/j.egypro.2017.03.539>
6. Song X.G., Cui L, Park Y.C. (2010) Three-dimensional CFD analysis of a spring-loaded pressure safety valve from opening to re-closure. In: Proceedings of the ASME 2010 Pressure Vessels and Piping Division/K-PVP Conference, Washington, DC. <https://doi.org/10.1115/PVP2010-25024>
7. Shiao Y, Kantipudi MB, Yang TH (2019) Performance estimation of an engine with magnetorheological variable valve train. *Adv Mech Eng* 11(5):1–11. <https://doi.org/10.1177/1687814019847795>
8. Xie H, Liu J, Yang H, Hu L, Fu X, Fan Y (2015) Design of pilot-assisted load control valve with load velocity control ability and fast opening feature. *Adv Mech Eng* 7(11):1–9. <https://doi.org/10.1177/1687814015618641>
9. Muller MT, Fales RC (2008) Design and analysis of a two-stage poppet valve for flow control. *Int J Fluid Power* 9(1):17–26. <https://doi.org/10.1080/14399776.2008.10781293>
10. Wang H, Chen Z, Huang J, Quan L, Zhao B (2022), Development of high-speed on-off valves and their applications. *Chin J Mech Eng* 35. <https://doi.org/10.1186/s10033-022-00720-5>
11. Wang B, Liu H, Hao Y, Quan L, Li Y, Zhao B (2021) Design and analysis of a flow-control valve with controllable pressure compensation capability for mobile machinery. *IEEE Access* 9:98361–98368. <https://doi.org/10.1109/ACCESS.2021.3095402>
12. Zhang X, Zhu Z, Xiang N, Ni Z (2016) A microfluidic gas damper for stabilizing gas pressure in portable microfluidic systems. *Biomicrofluidics* 10(5):054123. <https://doi.org/10.1063/1.4966646>. 1-10
13. Wang C, Quan L, Ou H (2019) The method of restraining hydraulic impact with active adjusting variable damping. *Proc Inst Mech Eng C J Mech Eng Sci* 233(11):3785–3794. <https://doi.org/10.1177/0954406218809740>
14. Ren F, Liu X, Chen J, Zeng P, Liu B, Wang Q (2014) Dynamic characteristics analysis of power shift control valve. *Adv Mech Eng*. <https://doi.org/10.1155/2014/824853>
15. Changbin G, Zongxia J, Shouzhan H (2014) Theoretical study of flow ripple for an aviation axial-piston pump with damping holes in the valve plate. *Chin J Aeronaut* 27(1):169–181. <https://doi.org/10.1016/j.cja.2013.07.044>
16. Zeng Q, Tian M, Wan L, Dai H, Yang Y, Sun Z, Lu Y, Liu F (2020) Characteristic analysis of digital large flow emulsion relief valve. *Math Probl Eng* 2020. <https://doi.org/10.1155/2020/5820812>
17. Qian J, Wu J, Gao Z, Jin Z. (2020) Pilot pipe and damping orifice arrangements analysis of a pilot-control globe valve. *J Fluids Eng* 142(10). <https://doi.org/10.1115/1.4047533>
18. Zhang J, Wang D, Xu B, Gan M, Pan M, Yang H (2018) Experimental and numerical investigation of flow forces in a seat valve using a damping sleeve with orifices. *J Zhejiang Univ Sci A* 19:417–430. <https://doi.org/10.1631/jzus.A1700164>
19. Jang S. C, Kang J. H. (2017). Orifice design of a pilot-operated pressure relief valve. *J Press Vessel Technol* 139(3). <https://doi.org/10.1115/1.4034677>
20. Zhang J, Yin W, Shi Y, Gao Z, Pan L, Li Y. (2022) Effects of the damping parameters on the opening and closing characteristics of vent valves. *Appl Sci* 12(10). <https://doi.org/10.3390/app12105169>
21. Chapra SC, Canale RP (2010) Numerical methods for engineers. The Mc-Graw Hill Companies, New York

### Publisher's Note

Springer Nature remains neutral with regard to jurisdictional claims in published maps and institutional affiliations.